Supplementary Information (SI) for Chemical Science.

Supporting Information: Modeling Catalytic Reaction on Ligand-protected Metal Nanoclusters

Vikas Tiwari and Tarak Karmakar*

Department of Chemistry, Indian Institute of Technology, Delhi, 110016 New Delhi, India

E-mail: tkarmakar@chemistry.iitd.ac.in

Phone: +91 11 2654 8549

Contents

1 Classical simulation details

1.1 Force field details

The initial structure of ligands and solvents were build using Avogadro software.[S1] The NanoModeler server[S2,S3] was used to produce the complete structure and topology of the nanocluster. NanoModeler employs the bonded parameters for gold-sulfur motifs developed by Pohjolainen et al.[S4] and non-bonded parameters developed by Heinz et al.[S5] Whereas, for ligands (DOP-SH and PET) and solvents ($CHCl_3$ and DMF), the general AMBER force field (GAFF)[S6] was used.

1.2 System setup and simulation details

All the classical MD simulations were performed using GROMACS version 2021.4,[S7] patched with PLUMED version 2.8.0.[S8,S9] The systems were first minimized using the steepest descent algorithm, followed by thermal equilibration at 300 K in the canonical (NVT) ensemble. Subsequently, isothermal-isobaric (NPT) simulations were conducted for equilibration of pressure. The NVT and NPT MD simulations were carried out for 250 ps and 1 ns respectively, with a time step of 0.5 fs, using a Leap-Frog integrator. The stochastic velocity rescaling thermostat[S10] with a temperature coupling constant of 0.5 ps was used for both NVT and NPT equilibration. In the case of NPT equilibration and production simulation, the system pressure was maintained at 1 bar, and the volumes were equilibrated using an isotropic Parrinello-Rahman barostat.[S11] The Particle Mesh Ewald (PME) method, with a grid spacing of 0.16 and an order of 4, was used to compute long-range electrostatic interactions. A cutoff of 1.0 nm was applied for both van der Waals and short-range Coulombic interactions. The partial-Mesh-Ewald method was utilized for treating long-range electrostatic interactions. For the production NPT simulations, each system was simulated with a time step of 2 fs. The LINCS algorithm[S12] was used to constrain all covalent bonds involving hydrogen atoms during the production runs.

1.2.1 Ligand dynamics

To understand the ligand dynamics, two systems were prepared with Au_{25}(S-DOP)$_{18}$ in $CHCl_3$ and DMF. For both the systems a cubic box of length 6 nm was used and the number of solvent molecules were added according to the their densities ($CHCl_3$ = 1.49 g/mL, DMF = 0.944 g/mL).

To assess the stability of the MPC's gold core, an Au-Au distance analysis was conducted. Distances between Au atoms in surface (AU-AUS) and ligand (AU-AUL) environments were calculated, and the average values were plotted using a kernel density estimate (KDE) in Figure S1.

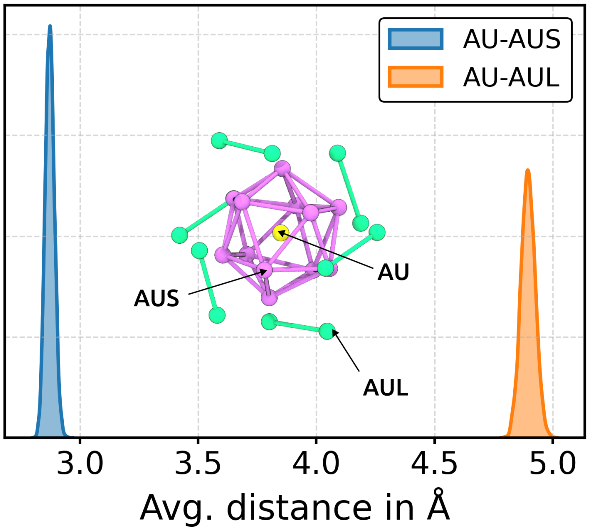

Figure S1: KDE plot showing average AU-AUS and AU-AUL distance.

1.2.2 Substrate binding

To understand the substrate binding, three systems were prepared: Au_{25}(S-DOP)$_{18}$ in $CHCl_3$, Au_{25}(S-DOP)$_{18}$ in DMF, and Au_{25}(PET)$_{18}$ in $CHCl_3$, each containing a single substrate. To accelerate the substrate binding event, on-the-fly probability enhanced sampling (OPES$_E$, where E stands for the explore variant) simulations were carried out. The distance between the centers of mass (COM) of the monolayer-protected cluster (MPC) and the substrate was used as the collective variable (s), with an adaptive Gaussian width (Figure S2). The energy was regulated using a barrier height of 25 kcal/mol throughout the simulation.

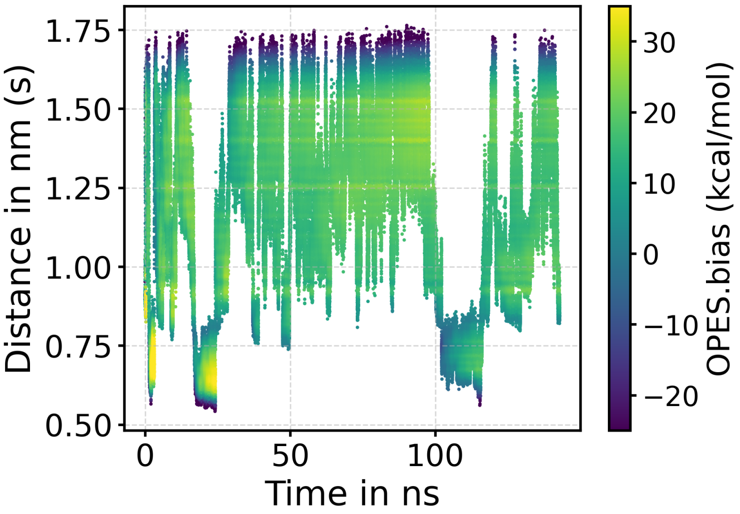

Figure S2: The CV profile shows the distance (s) between the centers of mass over simulation time for the OPES$_E$ simulation. The color bar indicates the amount of bias deposited during the simulation.

The active site for substrate binding exhibits a well-defined arrangement of gold atoms. The substrate interacts with a site consisting of six gold atoms: three inner gold atoms forming a triangle (orange) and three outer gold atoms forming a second triangle (pink) positioned above the inner triangle (Figure S3).

Subsequently, a set of 25 independent unbiased simulations were initiated from bound state to monitor the substrate's residence time for each system (Table S1). Committor analysis was conducted on-the-fly to terminate the simulation as soon as the substrate left the binding site. This approach ensured a comprehensive understanding of the substrate binding behavior across different systems and provided insights into the most favorable binding sites and residence times.

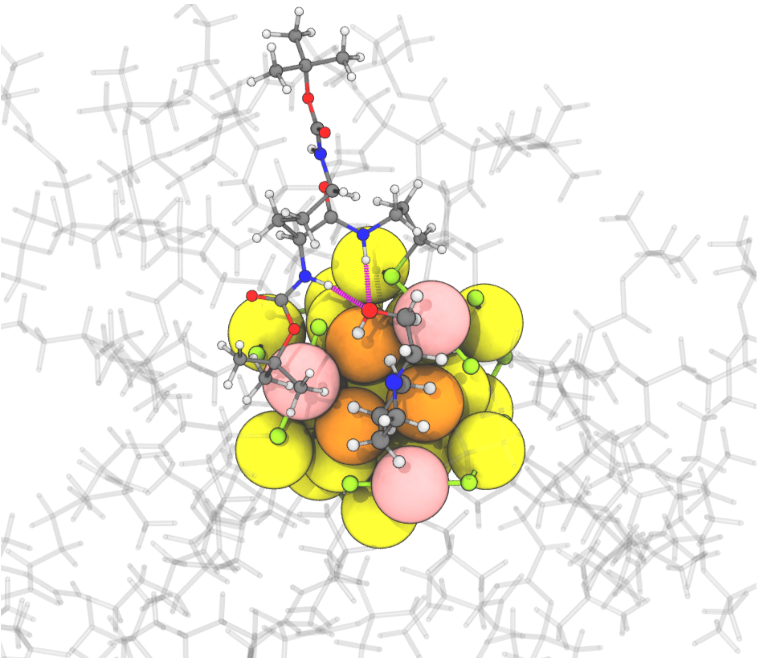

Figure S3: The substrate adsorbs onto the active site, which consists of three inner gold atoms (orange) and three outer gold atoms (pink).

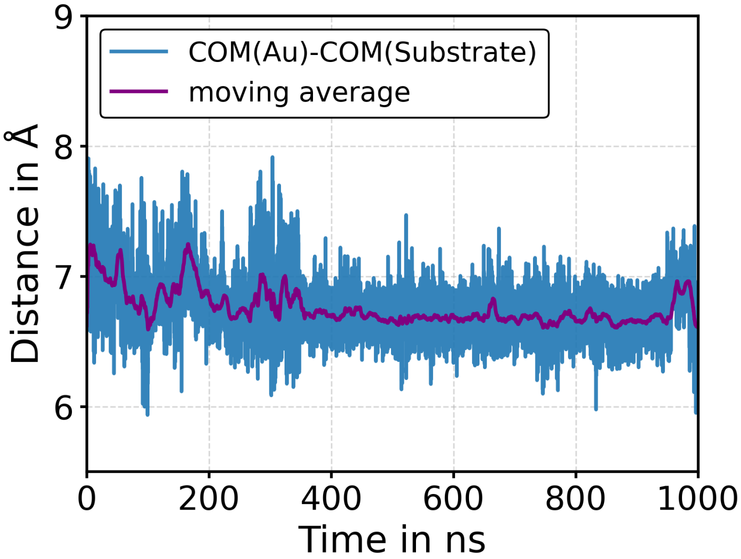

Figure S4: Time evolution of distance between COM of Au and COM of substrate.

Table S1: Substrate's residence time in ns

Simulation no.	**Au-DOP-$CHCl_3$**	**Au-DOP-DMF**	**Au-PET-$CHCl_3$**
1	100	1.5	11.2
2	100	2.4	13.4
3	31	2.1	7.8
4	100	6.3	2.6
5	100	4.7	14.5
6	100	1.7	37.1
7	100	10.0	8.7
8	72	7.0	1.9
9	100	2.1	12.2
10	100	3.8	7.6
11	100	2.1	3.4
12	100	2.1	33.8
13	100	3.1	14.6
14	100	0.7	15.5
15	100	1.1	13.5
16	100	1.5	10.7
17	55	2.2	13.9
18	45	2.9	13.3
19	100	1.6	16.4
20	19	9.6	15.7
21	100	1.5	3.6
22	5	0.4	17.2
23	100	2.1	2.2
24	100	2.2	3.9
25	100	4.1	5.2
Mean	**85**	**3**	**12**

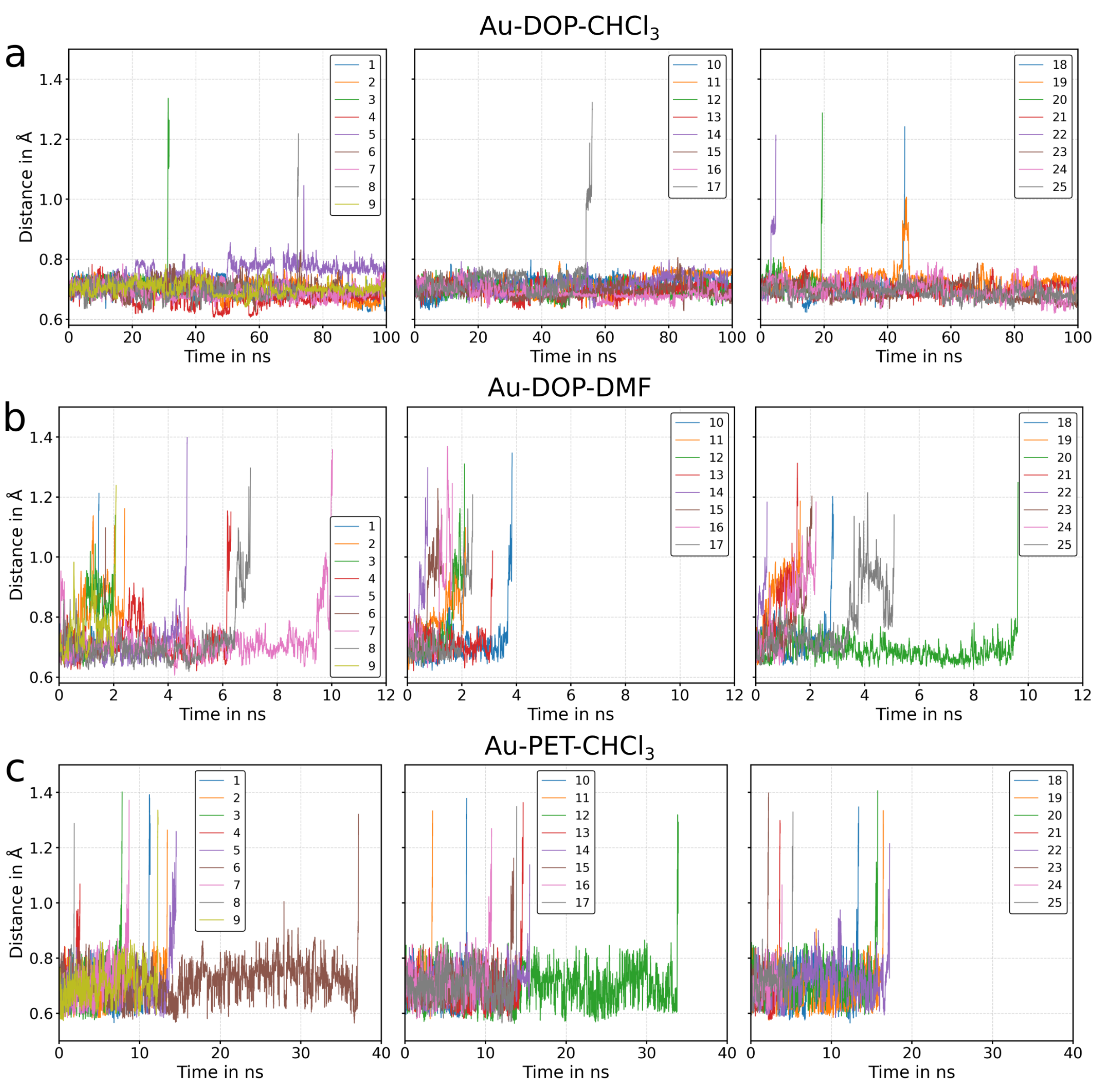

Figure S5: Time evolution of the center-of-mass (COM) distance between the substrate and nanocluster for (a) Au-DOP-CHCl$_3$, (b) Au-DOP-DMF, and (c) Au-PET-CHCl$_3$.

2 QM/MM simulation details

2.1 System setup and simulation details

The configuration of the bound state from the classical simulation was chosen as the starting point for the QM/MM simulation. All QM/MM simulations were performed using CP2K version 2022.1[S13] patched with PLUMED version 2.9.0.[S8,S9] In CP2K, the QM module QuickStep[S14] and MM module FIST were used. Equilibration as well as the production run for all QM/MM simulations was performed in the NVT ensemble with a time step of 0.5 fs. Temperature control was maintained using a Nose-Hoover thermostat with coupling constants set to 0.1 ps. For QM/MM electrostatic coupling, the Gaussian-smeared potential was used. The total cell length was maintained at 60.1 Å for all calculations. More details on QM/MM systems simulation are given in table S2.

Table S2: QM/MM simulation setup

Sr. no.	level of theory	QM type	atoms in QM	QM cell length
1	BLYP-D3(BJ)/DZVP	small	23	12 Å
2	BLYP-D3(BJ)/DZVP	large	70	20 Å

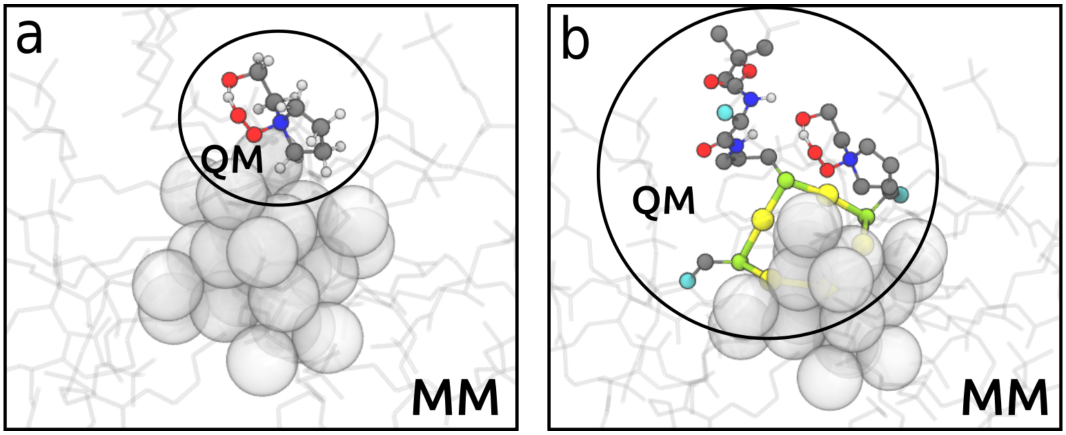

Figure S6: Representation of QM (colored atoms) and MM region for (a) small QM system and (b) larger QM system.

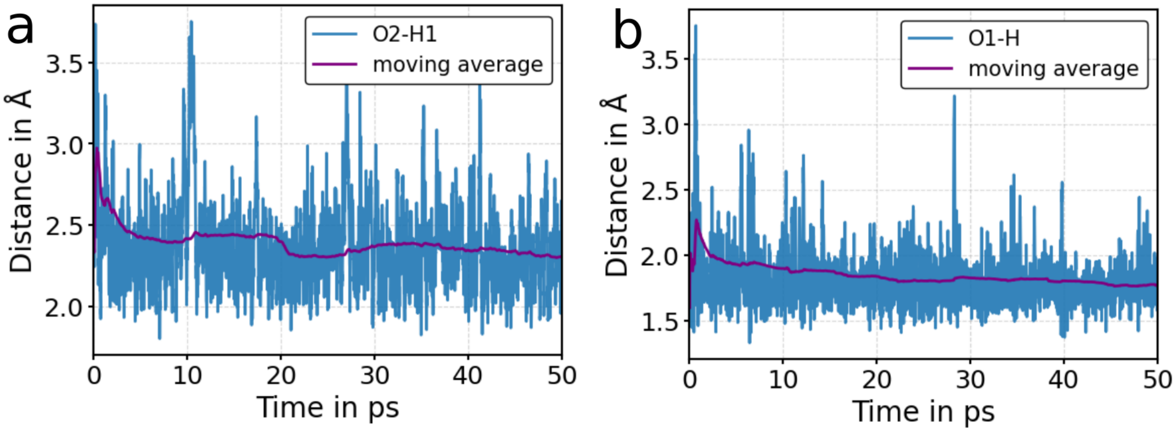

Figure S7: Time evolution of critical distances during unbiased QM/MM MD simulation: (a) distance between one of the oxygen atom O2 of the oxygen molecule and hydrogen H1 of the ligand (d_{O2-H1}), and (b) distance 2^{nd} oxygen atom O1 of the oxygen molecule and the substrate hydrogen (d_{O1-H}).

2.2 OPES simulation details

OPES[S15] metadynamics simulation were carried out to study the chemical reaction efficiently. The energy was regulated using a barrier height of 300 kJ/mol (71.70 kcal/mol) throughout the entire simulation time. In-built adaptive Gaussian width was used for all the simulations. The Gaussian hills were deposited every 20 simulation steps (10 fs). Path-based collective variable ($\sigma(\mathbf{d})$) was used to carry out the OPES metadynamics simulations which has been discussed in the manuscript. The CV profile for three independent set of simulations using small QM region and one simulation using large QM region are shown in Figure S8. The VMD software[S16] was employed to visualize simulation trajectories and prepare figures and movies. Analyses were performed using a combination of GROMACS in-built tools, PLUMED, and in-house written scripts.

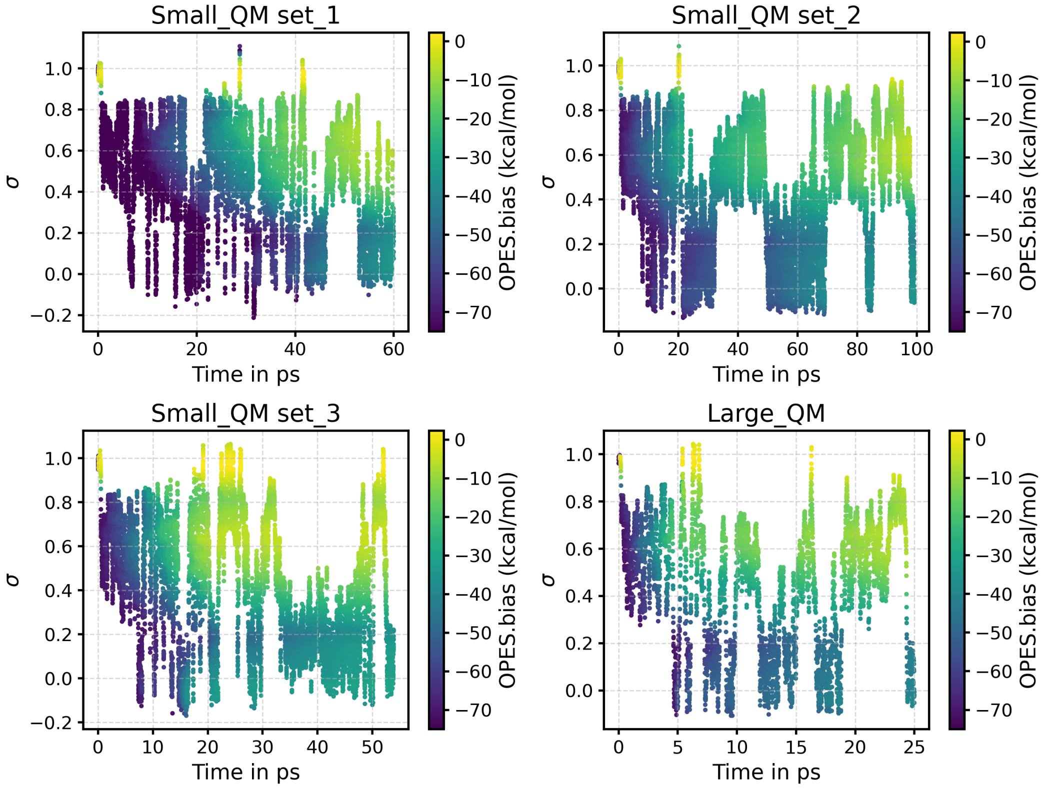

Figure S8: The variation of $\sigma(\mathbf{d})$ with simulation time (ps) for all four simulation sets is depicted, with colors representing the value of bias deposited in kcal/mol.

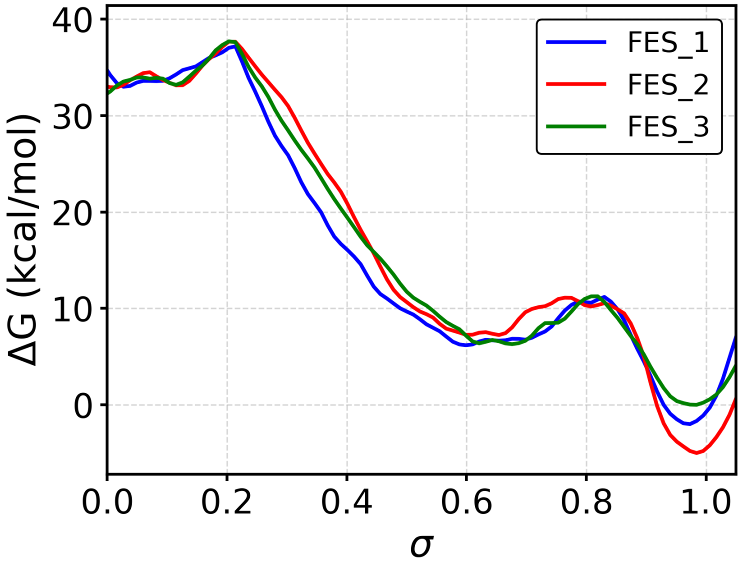

Figure S9: Free energy profile of all three independent simulations.

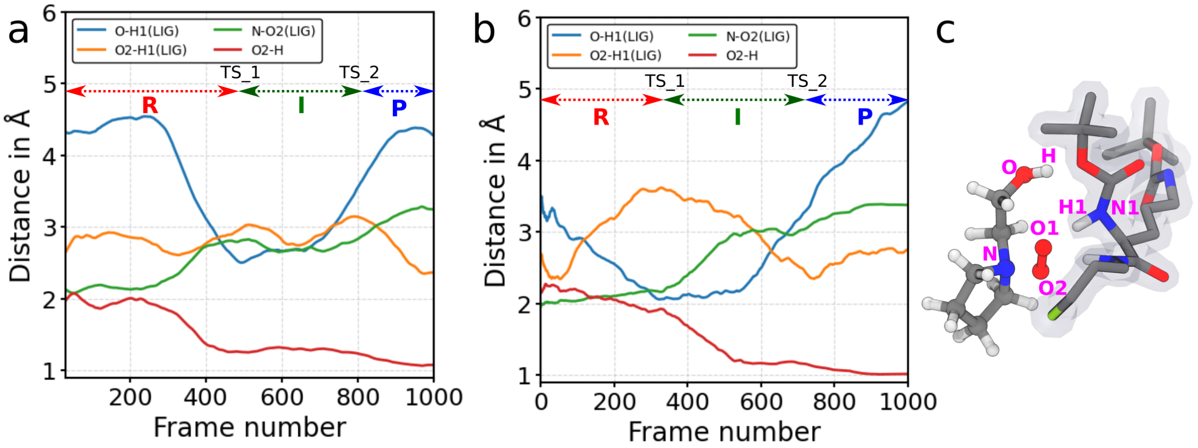

Figure S10: Evolution of key interatomic distances during the reactant-to-product transition computed for (a) the smaller QM region and (b) the larger QM region. Panel (c) presents a representative schematic with annotated atom names.

The convergence of OPES simulations was checked by calculating the difference in free energy between the reactant and product state (ΔG) with respect to simulation time (Figure S11).

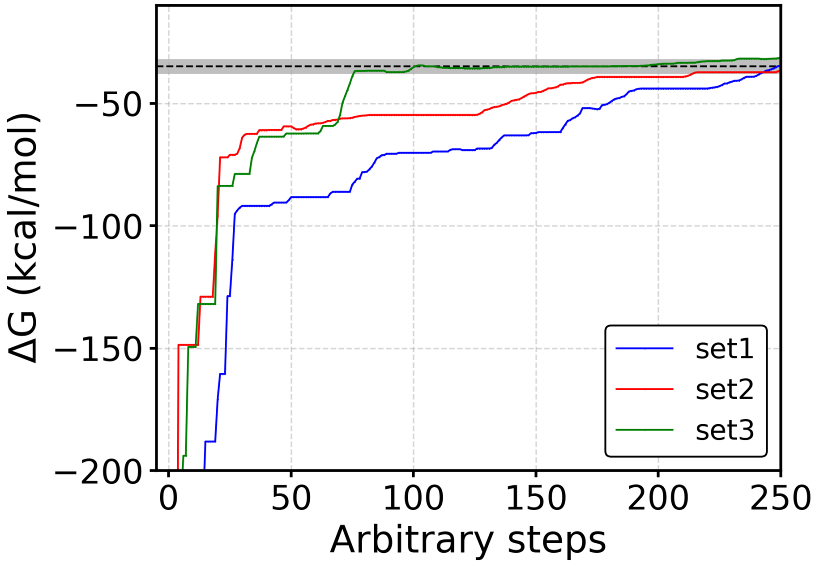

Figure S11: Evolution of ΔG (kcal/mol) with respect to the simulation time (ps).

2.3 QM/MM energy correlation (Au_5 vs Au_{25})

We selected 200 structures along the reaction pathway from the simulation, where 5 Au and 3 S atoms were initially included in the QM region. To refine the analysis, we expanded the QM region to encompass the entire $Au_{25}(SCH_2)_{18}$ cluster and recalculated the QM/MM energies. A correlation plot between the two sets of QM/MM energies revealed a moderate correlation, indicating consistency between the energy evaluations for the smaller and larger QM regions (Figure S12).

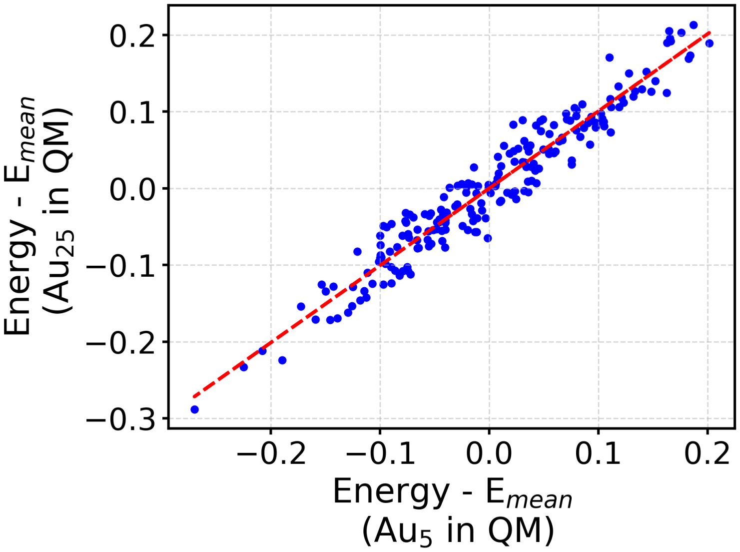

Figure S12: Scatter plot of QM/MM energy values with a linear correlation line. The x-axis and y-axis represent energies relative to their respective means for clarity. The dashed red line indicates the best-fit linear correlation.

References

(S1) Hanwell, M. D.; Curtis, D. E.; Lonie, D. C.; Vandermeersch, T.; Zurek, E.; Hutchison, G. R. Avogadro: an advanced semantic chemical editor, visualization, and analysis platform. *J. Cheminformatics* **2012**, *4*.

(S2) Franco-Ulloa, S.; Riccardi, L.; Rimembrana, F.; Pini, M.; Vivo, M. D. NanoModeler: A Webserver for Molecular Simulations and Engineering of Nanoparticles. *J. Chem. Theory Comput.* **2019**, *15*, 2022–2032.

(S3) Franco-Ulloa, S.; Riccardi, L.; Rimembrana, F.; Grottin, E.; Pini, M.; Vivo, M. D. NanoModeler CG: A Tool for Modeling and Engineering Functional Nanoparticles at a Coarse-Grained Resolution. *J. Chem. Theory Comput.* **2023**, *19*, 1582–1591.

(S4) Pohjolainen, E.; Chen, X.; Malola, S.; Groenhof, G.; Häkkinen, H. A Unified AMBER-Compatible Molecular Mechanics Force Field for Thiolate-Protected Gold Nanoclusters. *J. Chem. Theory Comput.* **2016**, *12*, 1342–1350.

(S5) Heinz, H.; Vaia, R. A.; Farmer, B. L.; Naik, R. R. Accurate Simulation of Surfaces and Interfaces of Face-Centered Cubic Metals Using 12-6 and 9-6 Lennard-Jones Potentials. *J. Phys. Chem. C* **2008**, *112*, 17281–17290.

(S6) Wang, J.; Wolf, R. M.; Caldwell, J. W.; Kollman, P. A.; Case, D. A. Development and testing of a general amber force field. *J. Comput. Chem.* **2004**, *25*, 1157–1174.

(S7) Berendsen, H.; van der Spoel, D.; van Drunen, R. GROMACS: A message-passing parallel molecular dynamics implementation. *Comput. Phys. Commun.* **1995**, *91*, 43–56.

(S8) Tribello, G. A.; Bonomi, M.; Branduardi, D.; Camilloni, C.; Bussi, G. PLUMED 2: New feathers for an old bird. *Comput. Phys. Commun.* **2014**, *185*, 604–613.

(S9) Bonomi, M.; Branduardi, D.; Bussi, G.; Camilloni, C.; Provasi, D.; Raiteri, P.; Donadio, D.; Marinelli, F.; Pietrucci, F.; Broglia, R. A.; Parrinello, M. PLUMED: A portable plugin for free-energy calculations with molecular dynamics. *Computer Physics Communications* **2009**, *180*, 1961–1972.

(S10) Bussi, G.; Donadio, D.; Parrinello, M. Canonical sampling through velocity rescaling. *Chem. Phys.* **2007**, *126*.

(S11) Parrinello, M.; Rahman, A. Polymorphic transitions in single crystals: A new molecular dynamics method. *J. Appl. Phys.* **1981**, *52*, 7182–7190.

(S12) Hess, B.; Bekker, H.; Berendsen, H. J. C.; Fraaije, J. G. E. M. LINCS: A linear constraint solver for molecular simulations. *J. Comput. Chem.* **1997**, *18*, 1463–1472.

(S13) Kühne, T. D.; Iannuzzi, M.; Del Ben, M.; Rybkin, V. V.; Seewald, P.; Stein, F.; Laino, T.; Khaliullin, R. Z.; Schütt, O.; Schiffmann, F.; Golze, D.; Wilhelm, J.; Chulkov, S.; Bani-Hashemian, M. H.; Weber, V.; Borštnik, U.; Taillefumier, M.; Jakobovits, A. S.; Lazzaro, A.; Pabst, H.; Müller, T.; Schade, R.; Guidon, M.; Andermatt, S.; Holmberg, N.; Schenter, G. K.; Hehn, A.; Bussy, A.; Belleflamme, F.; Tabacchi, G.; Glöß, A.; Lass, M.; Bethune, I.; Mundy, C. J.; Plessl, C.; Watkins, M.; VandeVondele, J.; Krack, M.; Hutter, J. CP2K: An electronic structure and molecular dynamics software package - Quickstep: Efficient and accurate electronic structure calculations. *The Journal of Chemical Physics* **2020**, *152*.

(S14) VandeVondele, J.; Krack, M.; Mohamed, F.; Parrinello, M.; Chassaing, T.; Hutter, J. Quickstep: Fast and accurate density functional calculations using a mixed Gaussian and plane waves approach. *Computer Physics Communications* **2005**, *167*, 103–128.

(S15) Invernizzi, M.; Parrinello, M. Rethinking Metadynamics: From Bias Potentials to Probability Distributions. *J. Phys. Chem. Lett.* **2020**, *11*, 2731–2736.

(S16) Humphrey, W.; Dalke, A.; Schulten, K. VMD: Visual molecular dynamics. *J. Mol. Graph.* **1996**, *14*, 33–38.